

Supplement of Hydrol. Earth Syst. Sci., 21, 5863–5874, 2017
<https://doi.org/10.5194/hess-21-5863-2017-supplement>
© Author(s) 2017. This work is distributed under
the Creative Commons Attribution 3.0 License.



Supplement of

Global change in streamflow extremes under climate change over the 21st century

Behzad Asadieh and Nir Y. Krakauer

Correspondence to: Behzad Asadieh (basadieh@sas.upenn.edu)

The copyright of individual parts of the supplement might differ from the CC BY 3.0 License.

Supplementary Information

The average value of change in streamflow extremes for each GCM-GHM combination, under RCP8.5 and RCP2.6 warming scenarios, are presented individually in the Tables S2 and S3, respectively. It should be noted that the results presented in the Tables S2 and S3, if averaged over the models for each quadrant, may result in different values from the multi-model average values reported in the main text. For the values reported in the main text, the results are first averaged over the models for each grid cell to create a multi-model global matrix. The grid-cells are then averaged over each quadrant, weighted by grid cell area. Assignment of each grid cell to the specified quadrants is based on the multi-model averages. For any single model datasets, grid cells (especially the ones with small multimodel mean projected changes) may fall in different quadrants, due to the disagreement among the GCMs and GHMs on projection of changes.

Some ISI-MIP hydrological impact models do not simulate streamflow for some grid cells for which other models do. This is due to the differences in the utilized global river network. Hence, a minority of grid cells do not have data from all hydrological models. However, grid cells with less than 20 (out of 25) available models are excluded from the calculations.

The results presented in the main text are based on the 95th and 5th percentiles of streamflow. Maps of changes in the median of streamflow are also presented in this supplement, along with the maps of changes in 95th and 5th percentiles.

The two-sample t-test (Snedecor and Cochran, 1989) is used in this study to quantify the statistical significance level of difference between the means of the 20C and 21C streamflow time series:

$$T = \frac{\bar{Q}_{21C} - \bar{Q}_{20C}}{\sqrt{\frac{\sigma_{21C}}{N_{21C}} + \frac{\sigma_{20C}}{N_{20C}}}} \quad \text{Eq.S1}$$

where \bar{Q}_{21C} and \bar{Q}_{20C} are the mean (high or low) streamflow, σ_{21C} and σ_{20C} are the streamflow time series variances, and N_{21C} and N_{20C} are the streamflow time series sample sizes (equal to 30-years in this study), in 21C and 20C, respectively. The means are significantly different if the absolute value of T is larger than the critical value of the t-distribution with v degrees of freedom, with v in an equal variance assumption being equal to $N_{21C} + N_{20C} - 2$. The value of Q here can be P5 or P95, meaning that we have calculated the T based on the P5 time series in 20C and 21C, and similarly based on the P95 time series. The critical value is defined based on the confidence level of significance and sample size, and at 95% level for a sample size of 30 it is equal to 2.042. The percentage of land area with statistically significant change (at 95% confidence level) is reported in this study.

Supplementary References:

Schewe, J., Heinke, J., Gerten, D., Haddeland, I., Arnell, N. W., Clark, D. B., Dankers, R., Eisner, S., Fekete, B. M., Colón-González, F. J., Gosling, S. N., Kim, H., Liu, X., Masaki, Y., Portmann, F. T., Satoh, Y., Stacke, T., Tang, Q., Wada, Y., Wisser, D., Albrecht, T., Frieler, K., Piontek, F., Warszawski, L. and Kabat, P.: Multimodel assessment of water scarcity under climate change, Proc. Natl. Acad. Sci., 111(9), 3245–3250, doi:10.1073/pnas.1222460110, 2013.

Snedecor, G. W. and Cochran, W. G.: Statistical methods, 8thEdn, Iowa State University Press, Iowa., 1989.

Table S1. Main characteristics of the global hydrological models used in this study (obtained from Schewe et al., 2013). LW: downwelling long-wave radiation; LWn: net long-wave radiation; P: precipitation rate (rain and snow calculated in the model); Q: air specific humidity; R: rainfall rate; RH: relative humidity; S: snowfall rate; SP: surface pressure; SW: downwelling shortwave radiation; T: air temperature; Tmax(min): daily maximum (minimum) air temperature; W: wind speed.

Model name	Time step	Meteorological forcing	Energy balance	Evaporation scheme	Runoff scheme	Snow scheme	Vegetation dynamics	CO2 effect
DBH	1hour	P, T, W, Q, LW, SW, SP	Yes	Energy balance	Infiltration excess	Energy balance	No	Constant
LPJmL	Daily	P, T, LWn, SW	Yes	Priestley-Taylor	Saturation excess	Degree-day	Yes	Varying
Mac-PDM	Daily	P, T, W, Q, LWn, SW, SP	No	Penman-Monteith	Saturation excess, non-linear	Degree-day	No	No
PCR-GLO BWB	Daily	P, T	No	Hamon	Saturation Excess Beta Function	Degree-day	No	No
WBM	Daily	P, T	No	Hamon	Saturation Excess	Empirical temp and Precip-based formula	No	No

Table S2. Normalized change in high and low streamflow extremes, averaged for each quadrant. Results presented for each model under RCP8.5 scenario. The results can also be reverted to the relative change in percentage for more distinct comparison (Figure S1).

RCP8.5		Quad. 1. increased high extreme and decreased low extreme		Quad. 2. increased high and low extreme		Quad. 3. decreased high and low extreme		Quad. 4. decreased high extreme and increased low extreme	
GCM	GHM	Change in high ext.	Change in low ext.	Change in high ext.	Change in low ext.	Change in high ext.	Change in low ext.	Change in high ext.	Change in low ext.
GFDL-ESM2m	WBM	0.072	0.178	0.196	-0.291	-0.285	0.451	-0.105	-0.171
	MacPDM	0.056	0.108	0.152	-0.206	-0.167	0.294	-0.066	-0.189
	PCR-GLOBWB	0.076	0.175	0.150	-0.186	-0.235	0.393	-0.121	-0.172
	DBH	0.079	0.074	0.129	-0.214	-0.161	0.169	-0.101	-0.314
	LPJmL	0.079	0.191	0.129	-0.231	-0.161	0.405	-0.088	-0.251
HadGEM2-ES	WBM	0.091	0.287	0.306	-0.477	-0.271	0.496	-0.095	-0.246
	MacPDM	0.051	0.077	0.172	-0.224	-0.148	0.270	-0.080	-0.192
	PCR-GLOBWB	0.102	0.250	0.226	-0.292	-0.268	0.474	-0.142	-0.218
	DBH	0.103	0.087	0.166	-0.301	-0.153	0.203	-0.094	-0.415
	LPJmL	0.110	0.220	0.176	-0.267	-0.141	0.412	-0.096	-0.288
IPSL-CM5A-LR	WBM	0.095	0.226	0.278	-0.423	-0.357	0.563	-0.114	-0.201
	MacPDM	0.058	0.087	0.179	-0.216	-0.190	0.302	-0.066	-0.143
	PCR-GLOBWB	0.108	0.241	0.241	-0.254	-0.289	0.481	-0.155	-0.220
	DBH	0.112	0.081	0.200	-0.281	-0.191	0.200	-0.126	-0.444
	LPJmL	0.128	0.211	0.188	-0.278	-0.187	0.394	-0.110	-0.279
MIROC-ESM	WBM	0.092	0.215	0.267	-0.423	-0.340	0.527	-0.089	-0.204
	MacPDM	0.041	0.061	0.116	-0.134	-0.150	0.259	-0.038	-0.087
	PCR-GLOBWB	0.103	0.261	0.223	-0.270	-0.272	0.443	-0.137	-0.194
	DBH	0.101	0.089	0.173	-0.322	-0.180	0.182	-0.109	-0.397
	LPJmL	0.116	0.200	0.160	-0.299	-0.164	0.389	-0.104	-0.299
NorESM1-M	WBM	0.081	0.215	0.189	-0.345	-0.255	0.429	-0.082	-0.204
	MacPDM	0.038	0.063	0.111	-0.151	-0.127	0.218	-0.077	-0.111
	PCR-GLOBWB	0.072	0.210	0.152	-0.218	-0.219	0.377	-0.105	-0.191
	DBH	0.074	0.058	0.121	-0.202	-0.140	0.122	-0.072	-0.356
	LPJmL	0.077	0.201	0.120	-0.237	-0.133	0.309	-0.103	-0.244

Table S3. Normalized change in high and low streamflow extremes, averaged for each quadrant. Results presented for each model under RCP2.6 scenario. The results can also be reverted to the relative change in percentage for more distinct comparison (Figure S1).

RCP2.6		Quad. 1. increased high extreme and decreased low extreme		Quad. 2. increased high and low extreme		Quad. 3. decreased high and low extreme		Quad. 4. decreased high extreme and increased low extreme	
GCM	GHM	Change in high ext.	Change in low ext.	Change in high ext.	Change in low ext.	Change in high ext.	Change in low ext.	Change in high ext.	Change in low ext.
GFDL-ESM2m	WBM	0.067	0.143	0.153	-0.224	-0.153	0.270	-0.063	-0.134
	MacPDM	0.035	0.108	0.094	-0.137	-0.104	0.171	-0.032	-0.081
	PCR-GLOBWB	0.055	0.120	0.110	-0.173	-0.123	0.228	-0.065	-0.125
	DBH	0.046	0.037	0.086	-0.116	-0.077	0.068	-0.044	-0.128
	LPJmL	0.042	0.162	0.078	-0.158	-0.065	0.237	-0.045	-0.178
HadGEM2-ES	WBM	0.069	0.149	0.184	-0.297	-0.151	0.279	-0.062	-0.141
	MacPDM	0.031	0.052	0.097	-0.136	-0.068	0.125	-0.033	-0.072
	PCR-GLOBWB	0.072	0.154	0.141	-0.181	-0.145	0.271	-0.080	-0.143
	DBH	0.059	0.048	0.105	-0.142	-0.068	0.082	-0.044	-0.163
	LPJmL	0.073	0.165	0.106	-0.183	-0.061	0.233	-0.049	-0.182
IPSL-CM5A-LR	WBM	0.055	0.124	0.141	-0.235	-0.170	0.278	-0.088	-0.138
	MacPDM	0.033	0.054	0.082	-0.103	-0.088	0.140	-0.026	-0.071
	PCR-GLOBWB	0.055	0.131	0.108	-0.144	-0.161	0.274	-0.091	-0.149
	DBH	0.055	0.046	0.098	-0.142	-0.092	0.095	-0.045	-0.190
	LPJmL	0.060	0.165	0.084	-0.180	-0.078	0.251	-0.055	-0.162
MIROC-ESM	WBM	0.056	0.156	0.175	-0.263	-0.208	0.329	-0.063	-0.135
	MacPDM	0.031	0.040	0.073	-0.106	-0.074	0.126	-0.019	-0.047
	PCR-GLOBWB	0.063	0.159	0.146	-0.196	-0.176	0.289	-0.072	-0.135
	DBH	0.057	0.059	0.114	-0.157	-0.102	0.093	-0.074	-0.201
	LPJmL	0.063	0.172	0.091	-0.190	-0.094	0.272	-0.067	-0.184
NorESM1-M	WBM	0.045	0.116	0.129	-0.205	-0.147	0.235	-0.049	-0.112
	MacPDM	0.023	0.048	0.064	-0.082	-0.063	0.118	-0.024	-0.054
	PCR-GLOBWB	0.051	0.124	0.087	-0.129	-0.133	0.239	-0.054	-0.112
	DBH	0.050	0.036	0.069	-0.114	-0.082	0.068	-0.036	-0.122
	LPJmL	0.041	0.155	0.062	-0.145	-0.056	0.211	-0.048	-0.149

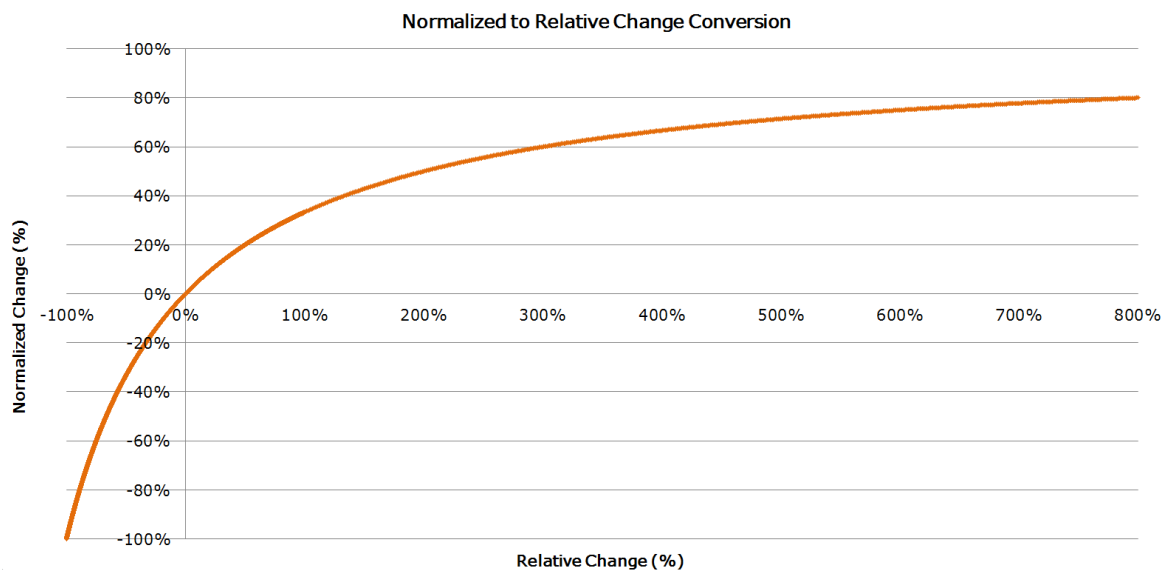


Figure S1. Normalized change (in %; values calculated by equation 1 multiplied by 100) versus relative change (%) curve.

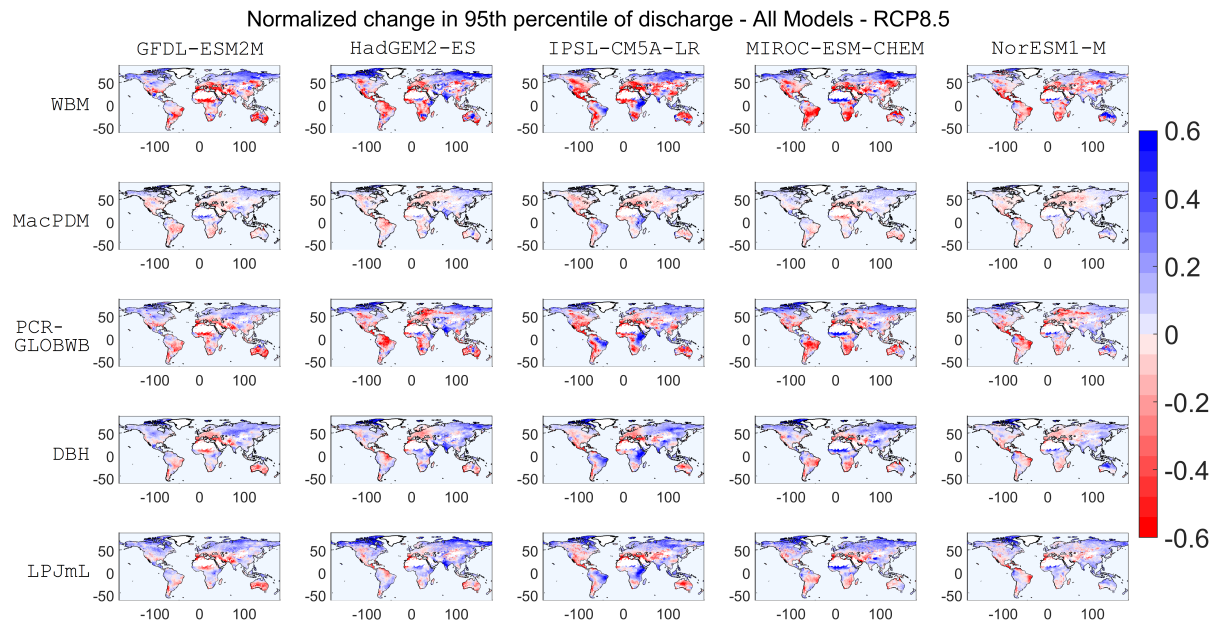


Figure S2. Normalized change in P95 for each of GHM/GCM combinations under RCP8.5 scenario.

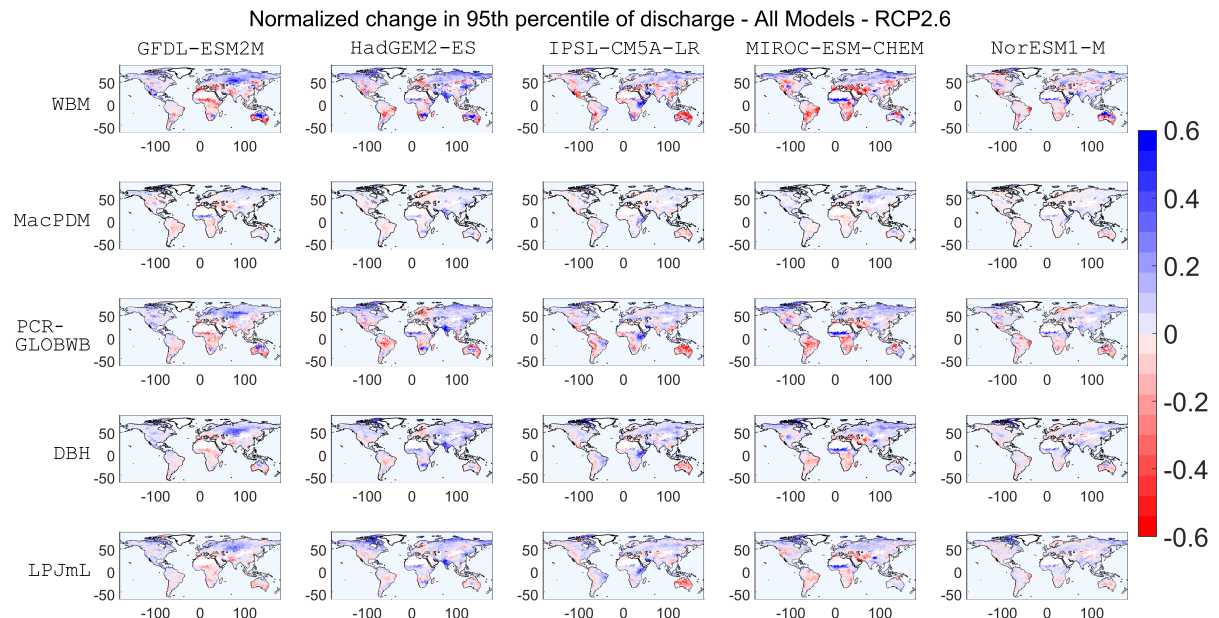


Figure S3. Normalized change in P95 for each of GHM/GCM combinations under RCP2.6 scenario.

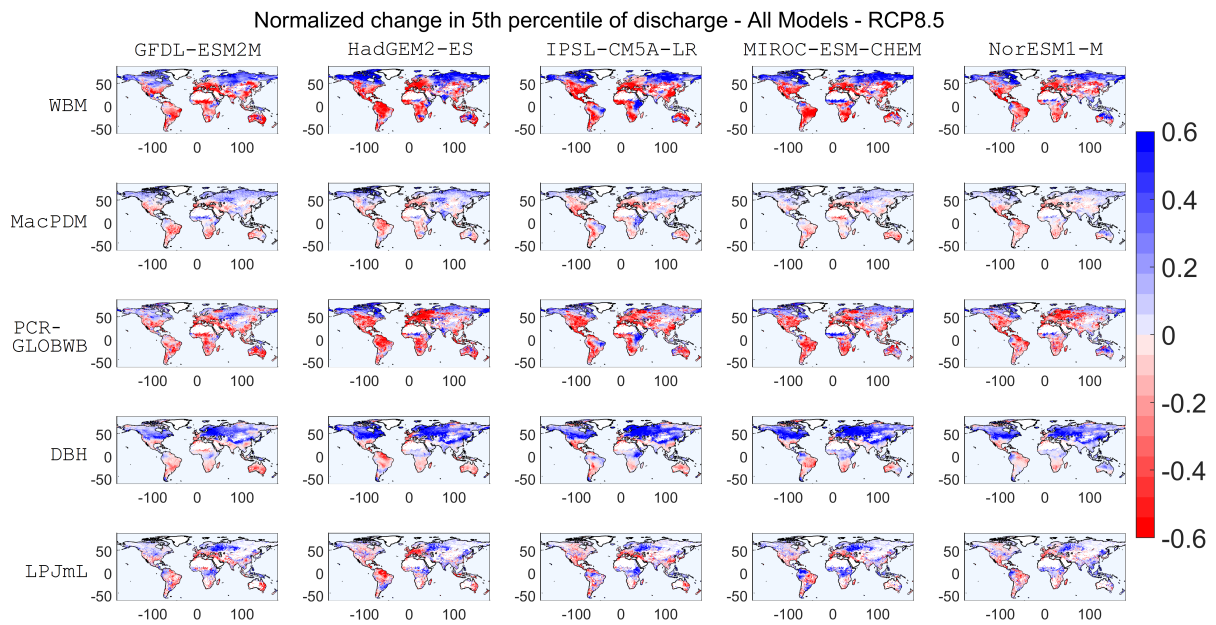


Figure S4. Normalized change in P5 for each of GHM/GCM combinations under RCP8.5 scenario.

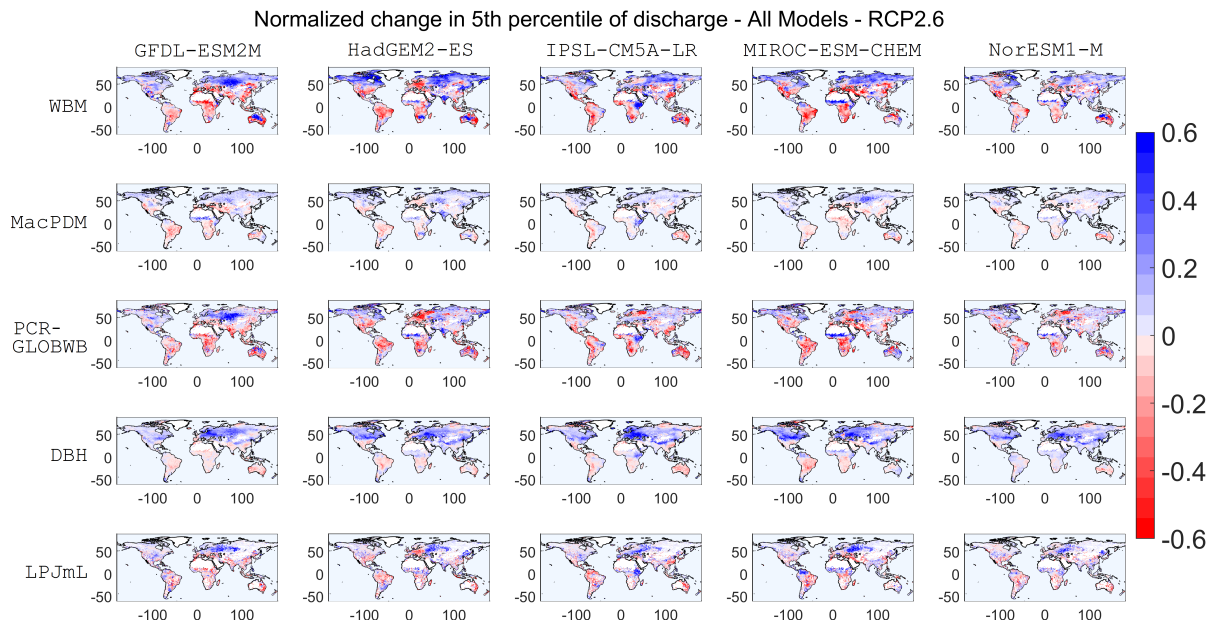


Figure S5. Normalized change in P5 for each of GHM/GCM combinations under RCP2.6 scenario.

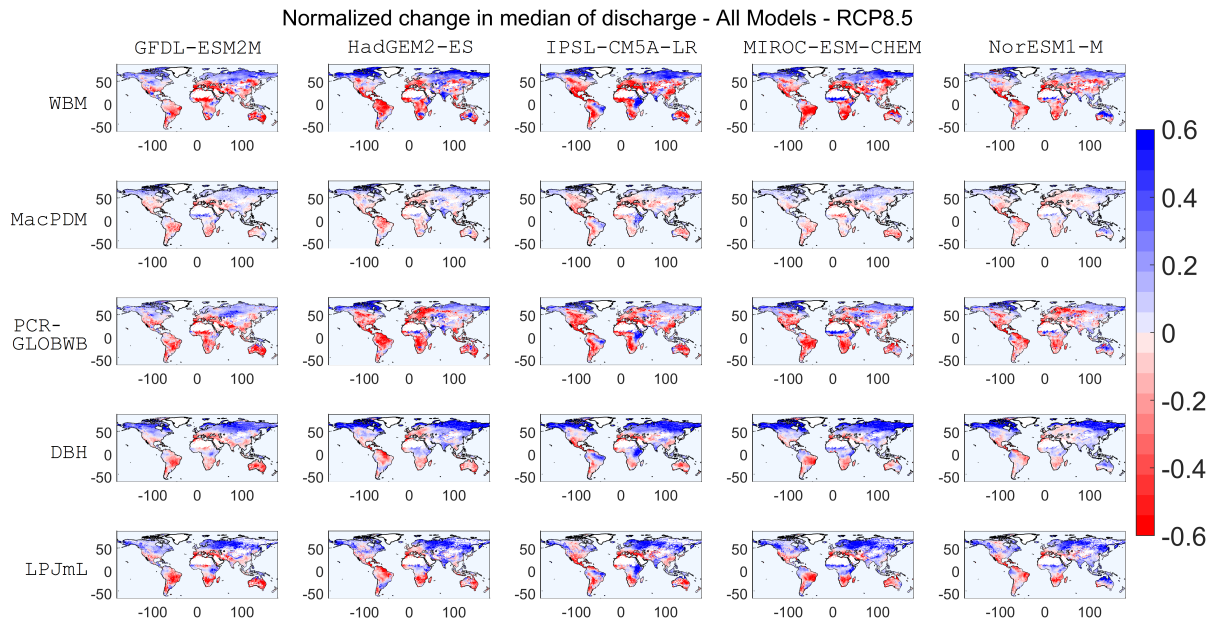


Figure S6. Normalized change in median of streamflow for each of GHM/GCM combinations under RCP8.5 scenario.

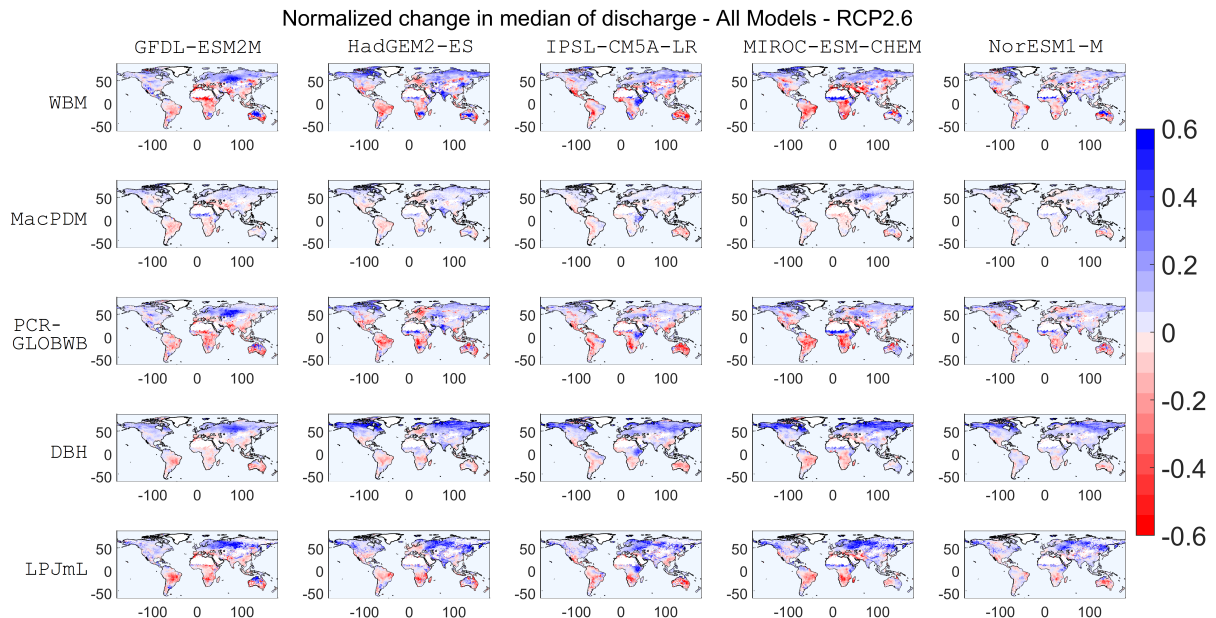


Figure S7. Normalized change in median of streamflow for each of GHM/GCM combinations under RCP2.6 scenario.